An Analytical and Experimental Study of the Linear Fresnel Reflector Solar Concentrator System

R. Manikumar and A. Valan Arasu

ABSTRACT

A solar hot water generation system that makes use of a linear Fresnel reflector solar concentrator (LFRSC) technique to concentrate solar radiation onto a stationary absorber cavity suspended above the concentrator plane is proposed. Heat loss from the trapezoidal cavity absorber occurs via a complex interaction between radiation, convection and conduction within the cavity, and then from cavity to the surroundings. This article describes and compares experimental and analytical methods used to investigate the heat losses from the cavity absorbers with and without plate underneath the absorber tubes. Reasonable agreement is achieved between the two methods for heat loss in the cavity absorber. Also, analytical and experimental thermal performance analysis of LFRSC system is determined. The results are presented and discussed.

Keywords: LFRSC, analytical model, trapezoidal cavity absorber, overall heat loss coefficient.

Nomenclature

A_a Aperture area of the concentrator [m^2]
A_c Area of the transparent glass cover placed at the bottom [m^2]
A_p Absorber plate area [m^2]
A_r Absorber tubes surface area [m^2]
c Specific heat of the water [kJ/kgK]
C Constant used to find Nusselt number
CP Total concentrated power on the tubular absorber [W]
CR Concentration ratio
D_e Distance between the absorber surface and transparent cover [mm]
f Focal height of the absorber [m]

Gr	Grashof number
h_{co}	Convection heat loss coefficient from the bottom glass surface [W/m^2-K]
h_{cp}	Convection heat loss coefficient from the absorber surface [W/m^2-K]
h_{ro}	Radiation heat loss coefficient from the bottom glass surface [W/m^2-K]
h_{rp}	Radiation heat loss coefficient from the absorber surface [W/m^2-K]
h_w	Heat loss coefficient from the transparent cover to the surroundings [W/m^2-K]
I	Direct component of solar flux [kW/m^2]
L	Length of the absorber [m]
N	Total number of reflector on either side of the central reflector of the concentrator.
Nu_{cp}	Nusselt number
n	Reflector position number on either side of the central reflector of the concentrator
P_n	Solar power on the tubular absorber contributed from the nth reflector [W]
Pr	Prandtl number
R	Location of constituent mirror elements [m]
s	Shift between the mirror elements [m]
T_a	Ambient temperature [°C]
T_c	Cover temperature [°C]
T_i	Water inlet temperature [°C]
T_o	Water outer temperature [°C]
T_p	Absorber plate temperature [°C]
T_s	Absorber tube surface temperature [°C]
T_{tank}	Storage tank temperature [°C]
U_l	Overall heat loss coefficient [W/m^2°K]
w	Width of the reflector [m]
W	Width of the absorber plane [mm]
W_g	Width of the glass cover [mm]
z	constant used to find Nusselt number

Greek Symbols

ϱ	Specular reflectance of the glass reflector
θ_n	Tilt of the nth reflector [°]

ε Half of the angular subtense of the sun at any point on the earth [=16′]
ε_p Emissivity of the absorber surface
ε_c Emissivity of the transparent cover
σ Stefan Boltzman constant

INTRODUCTION

A linear Fresnel reflector solar concentrator system is a solar concentrating system where stripes of mirrors at ground level rotate around independent parallel axes to reflect sunlight on an elevated, fixed linear absorber. The concept has been proposed initially as an alternative to tower systems with heliostat fields [1], a large Fresnel linear collecting field would have concentrated the sunlight on a unique linear absorber, on a high support (61 m). However, the comparison with central tower systems seemed unfavourable [2], the incident light is less efficiently exploited (the tracking is on one axis) due to the lower concentration factor and a linear receiver has greater heat losses than a central receiver. The cost of the LFRSC manufacture and maintenance are presumably lower. The two-stage linear Fresnel reflector solar concentrator was analyzed via an in-depth study of an installed, nominally 220 kWt systems. The principal practical design options for the secondary concentrator were evaluated via a computer simulation which includes ray-tracing of the reflectors. The Fresnel concentrator can be considerably less expensive [3] than the corresponding parabolic trough collector, but was found to deliver about one-fourth less yearly energy. However, much of this difference could be eliminated through the use of higher-quality CPC reflectors [4,5]. The LFRSC field can be imagined as a broken-up parabolic trough reflector [6]. However unlike parabolic troughs, the mirrors used for reflection are flat in shape. The greatest advantage of this type of system is that the used flat mirrors are cheaper than parabolic glass reflectors. Additionally, these are mounted close to the ground, thus minimizing structural requirements [7]. In Australia, a Fresnel system has been built to be integrated with the Liddell coal plant; it uses slightly bent mirrors without any secondary reflector near the absorber. Another prototype has been designed by the Solarmundo company [8], with a secondary reflector provided above the absorber serves also as a wind protection to reduce convective losses. At the Plataforma Solar

de Almeria (Spain), a Fresnel string based on the Solarmundo project [8] has been built. A 5MWprototype [9] has been built in California by Ausra company, which has also proposed a full-scale 177 MW plant (the Carrizo Energy Solar Farm Project). Simulations and studies have been performed on the properties of an elevated linear absorber [10] and storage systems have been proposed [11]. A preliminary economical analysis [12] shows that the system should produce electric energy cheaper than trough plants of the SEGS model. The receiver is nothing but a stationary linear cavity, usually trapezoidal, consisting of a number of tubes. The inside of the cavity, external to the tubes contains air which is not in contact with ambient. The tubes are heated by absorbing reflected solar radiation from the LFRSC field placed on the ground. The water flowing through the tubes inside the cavity absorbs heat. A linear Fresnel reflector solar concentrator with a cavity absorber can provide operating temperatures in the range of 70 – 200°C [6].

Heat loss from the absorber tube occurs by a complex mechanism that includes all the three modes of heat transfer namely radiation, convection and conduction modes. The knowledge about that loss through the structure surrounding the absorber tubes is very important because it affects the efficiency of the collecting system. The heat loss depends on several factors, as the geometry of the cavity, absorber tubes (with and without plate), distance between the adjacent absorber tubes, material selection etc. The study [13] demonstrated that the heat losses from the cavity are predominantly by radiation as compared to convection heat losses. Singh et al. [14] studied the performance of round and rectangular pipe absorber experimentally. They concluded that the efficiency of the round pipe (multi-tube) absorber was 2-8% higher as compared to rectangular pipe absorber. Also the efficiency of the rectangular pipe absorber ranged from 24% to 63% for selective surface coated absorber as compared to 15% to 54% with ordinary black painted absorber at different concentration ratios. Similarly, efficiency of the selective surface coated round pipe absorber varied from 25.7% to 71.2% as compared to 16% to 59.6% for ordinary black painted round pipe absorber. Flores Larsen et al. [15] analyzed the steady state thermal behavior of an absorber in the LFRSC system by using Energy Plus software package and concluded that the higher portion of the thermal loss occurs by radiation from the window surface, that is, for a pipe temperature of 200°C around 91% of the heat is lost from the bottom glass cover. Also, the overall heat loss coefficient of the absorbers increased with absorber temperature in

all cases considered and also selective surface coating on the absorber found useful as compared to ordinary black paint because there was significant reduction in overall heat loss coefficient by 20-30% [16]. In the study of the trapezoidal cavity [17], it was found that non-uniform heating of the bottom wall produced greater heat transfer rate as compared to uniform heating case for the Rayleigh number in the range of 103 to 105. Radiation heat transfer coefficient between hot absorber plate and glass cover of the cavity can be calculated considering radiative heat transfer modeled as that between two parallel planes [18]. Considering emissivities of the hot and cold plates and interaction of surface radiation with free convection [19], correlations were developed for square cavity with air as the intervening medium. A new trapezoidal cavity receiver for a LFRSC was analyzed and optimized via ray trace and CFD simulations [20]. The computational study of heat loss characteristics by using non-Boussinesq numerical procedure in CFD package with FLUENT version 6.3 has been developed [21] and concluded that trapezoidal cavity absorber with aspect ratio (depth to width of the cavity) is greater than 2.5 and temperature ratio (cover to hot surface temperature) greater than 0.6 can be used to minimize the internal heat loss of the absorber. Also, numerical comparative study of combined natural convection (incorporating Boussinesq approximation) and surface radiation model for the same two solar trapezoidal cavity absorber models (with and without plate) of LFRSC system was carried out by the same authors [22] by using ANSYS workbench FLUENT [23] module (computational) and MATLAB simulation program (analytical). A good agreement between analytical and CFD simulated models were observed (within ±20%).

For a large-scale practical harnessing of any renewable energy technology, a detailed performance evaluation of energy conversion system model is necessary. Knowledge about the effect of various design parameters of the trapezoidal cavity absorber on thermal performance of the LFRSC (Fig. 1) model is important. To accomplish this, an experimental LFRSC model is developed to study the effect of absorber surface temperature, cavity absorber (with and without plate underneath the absorber tubes) and mass flow rate of working fluid (water in the present case) on its thermal performance. The first cavity model has absorber plate at the top of the cavity (with plate) and the second one has absorber tubes (without plate) at the top of the cavity. The above two cavity models are developed and the experimental results of them are compared with analytical results. Since, most of the published works have focused

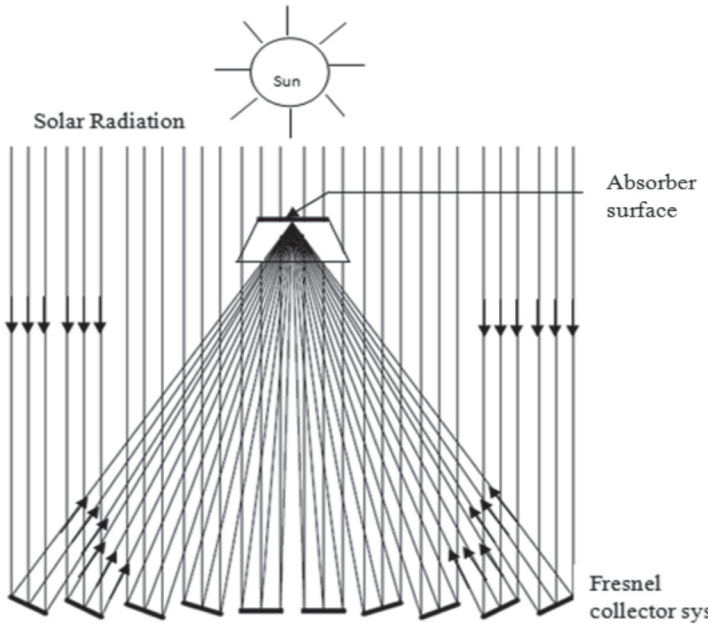

Figure 1. A schematic view of LFRSC with trapezoidal cavity absorber

on the plane absorber surface, the present analysis concentrates on the thermal performance comparison of trapezoidal cavity with plate underneath absorber tubes and without plate (absorber tubes only). Findings of the study are discussed in this article.

DESIGN OF LFRSC SYSTEM

Experimental set-up

The basic elements making up a conventional LFRSC are:

(i) the absorber tubes with and without plate underneath in a trapezoidal cavity
(ii) the transparent glass cover placed at the bottom of the absorber cavity
(iii) the reflector
(iv) the support structure.

Elements (i) and (ii) together constitute the main trapezoidal absorber cavity, while elements (iii) and (iv) constitute the concentrator.

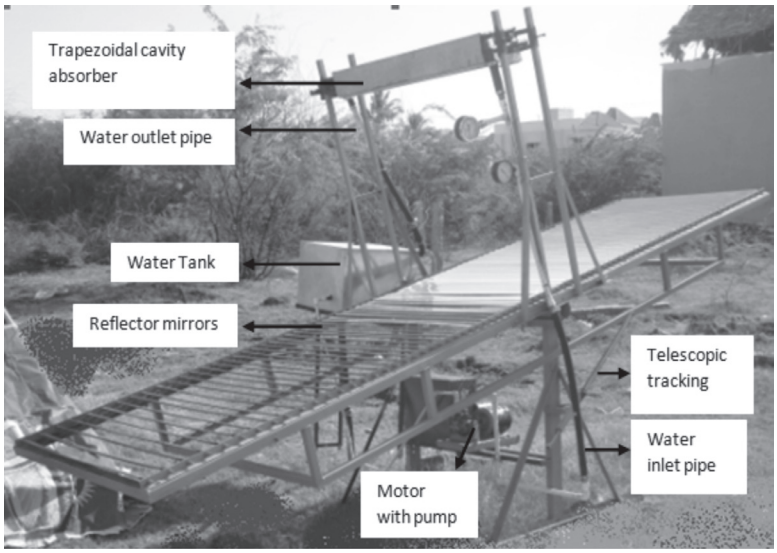

Figure 2. Experimental set-up of LFRSC with trapezoidal cavity absorber

Following assumptions are made to facilitate the designing of LFRSC (i) the reflector elements are specularly reflective and (ii) the solar radiation incident normally on the reflector elements. An experimental set-up of LFRSC system is shown in Figure 2. It consists of 2N reflector elements, with N (in the present system, N = 40) reflectors present on either side from the centre of the concentrator plane, water tank, cavity absorber set up with thermocouples, flow regulator and water circulation pump. The solar concentrator consists of 40 reflecting units on either side of absorber, each having 1000 mm length and 40 mm width fixed onto a rectangular frame (1050 mm length and 4100 mm width). Each mirror reflector was fixed separately at the required angle, corresponding to the noon condition, to focus sun rays at the absorber. Solar concentrator frame is provided with a telescopic pipe arrangement to keep the whole reflecting unit at the required slope so that sun rays could fall perpendicular to the absorber plane. The Fresnel concentrator axis is oriented along the N-S direction. The frame is moved in the E-W direction with great care at every 15 minutes and reading is taken at the interval of every 1 hour. The water is heated when it flows through the trapezoidal cavity absorber tubes at a desired flow rate and fall into the tank again. The inlet header and outlet header are used to connect the absorber tubes. The inlet header is connected with pump and outlet header is connected with tank

through chlorinated polyvinyl chloride (CPVC) pipe and rubber hose of 12.5 mm ID. The dimension of water storage tank is 350 x 350 x 475mm by volume with glass wool insulation thickness of 150mm all around the sides. A flow regulator valve is fitted to control the water flow through the absorber tubes. Thermal performance of the two trapezoidal cavity absorbers with and without plate of linear Fresnel solar concentrating collector is studied experimentally in the outdoor conditions.

Calibrated k-type (make: LUTRON TM – 902C) digital thermocouple has been used to measure the absorber surface temperature, glass cover temperature and storage tank temperature. Also calibrated PT (RTD Type) – 100 sensor (make: SELECTRON 303) has been used to measure the outlet temperature of the water. Thermocouples are connected to a digital meter with LED display to record their outputs. The uncertainties in the measured data were calculated based on the procedure given by Singh et al. [14]. The uncertainty in measurement of temperature and solar intensity are ±0.25% and ± 5% respectively. The uncertainty in experimental overall heat loss coefficient for the cavity absorber was estimated about ±2%.

Design of Concentrator

The tilt of each mirror elements is chosen such that a ray incident normally on the aperture plane and striking the midpoint of the mirror element, after reflection, reaches the focal point. If absorber tubes are arranged horizontally along the absorber plane such that the centre of the absorber plane coincides with the point f, then the lower sides of the absorber tubes will be illuminated by the radiation reflected from the constituent mirror elements. Using simple geometrics optics, the tilt of the first mirror element with the concentrator plane can be calculated as [24],

$$\theta_1 = \frac{1}{2}\left[\tan^{-1}\left(\frac{R_1 + w/2\cos\theta_1}{f - w/2\sin\theta_1}\right)\right] \quad (1)$$

where, R1 is the location of the first mirror element on either half of the concentrator, w is the width of the constituent mirror elements and f (≈ 1.1m) is the distance between the centre of the absorber and the concentrator plane. The above implicit equation may be solved iteratively for θ_1. The location of the second mirror element and its tilt with the concentrator plane are chosen such that the radiation reflected from the second mirror element is not blocked by the first mirror element. This neces-

sitates introducing a certain space between two consecutive mirror elements. The necessary shift (s_n) for the second mirror element is given by:

$$s_1 = w\sin\theta_1 \tan(2\theta_2 + \varepsilon) \tag{2}$$

On the basis of similar geometrics optical considerations, the following generalized expressions for shift (s_n), location (R_n) and tilt (θ_n) parameters associated with the nth mirror element can be derived:

$$s_n = w\sin\theta_{n-1} \tan(2\theta_n + \varepsilon) \tag{3}$$

$$R_n = R_{n-1} + w\cos\theta_{n-1} + s_n \tag{4}$$

and $$\theta_n = \frac{1}{2}\left[\tan^{-1}\left(\frac{R_n + w/2\cos\theta_n}{f - w/2\sin\theta_n}\right)\right] \tag{5}$$

with $\theta_0 = 0$, $s_1 = 0$ and $R_0 = w/2$, $R_1 = w/2$ as initial values for iteration and n = 1,2,….,N.

By using the above equations, the values of θ_n, s_n and R_n are found out for each mirror elements. Each of the mirror elements is then locked into position, so that the axial mirrors produce an image of the sun on the lower side of the absorber.

Performance Parameters

Concentration ratio (CR) of the LFRSC is obtained by summing up the concentration contribution of the each reflector element. Contribution of concentration of nth reflector element (CI_n) to the local concentration ratio distribution on the absorber surfaces is calculated by,

$$CR = 2\sum_{n=1}^{N} CI_n \tag{6}$$

$$CI_n = w\cos\theta_n / G_n \tag{7}$$

$$I_n = [f - (w\sin\theta_n \sec 2\theta_n \sin\varepsilon)]/(\cos 2\theta_n - \varepsilon) \tag{8}$$

$$J_n = w\cos\theta_n \sec 2\theta_n \tag{9}$$

$$K_n = [(h \sec 2\theta_n \sin \varepsilon) / \cos(2\theta_n + \varepsilon)] \quad (10)$$

$$G_n = I_n + J_n + K_n \quad (11)$$

where I_n, J_n and K_n are width of the portion of reflected rays on the absorber surface.

In the Fresnel concentrator–tubular collector system, as different reflector elements reflect energy on to the absorber, it is more meaningful to determine the total concentrated power reaching the absorber. Solar power (P_n) reached to the absorber contributed from the nth reflector is given by [24],

$$P_n = \rho I w \cos\theta_n L \quad (12)$$

Thus, the total concentrated power on the receiver due to the contributions from all the reflector elements, including the central one is,

$$\mathrm{CP} = (2\sum_{n=1}^{N} \mathrm{P_n}) + \mathrm{P_c} \quad (13)$$

where,

$$P_c = \rho I (w - W_g) L \quad (14)$$

Note that the solar power P_c is equal to zero, if width (w) of the reflector is less than or equal to bottom width (W_g) of the trapezoidal cavity absorber.

Aperture diameter (D) is derived from the basic geometry and expressed as [25],

$$D = 2\left(R_n + w_n \cos\theta_n\right) \quad (15)$$

The aperture diameter of present LFRSC system is calculated as 4.0 m and so the total aperture area is approximately 4.0 m^2 as length of the system is 1m.

Efficiency of LFRSC System

The concentrator is oriented in N-S horizontal and E-W tracking configuration. The thermal efficiency test for each concentrator-absorber

(with and without plate) system is conducted for different surface temperature and various mass flow rates. A proper record of inlet and outlet water temperatures, absorber surface temperature, tank water temperature and mass flow rate of water is made. The thermal efficiency (η) is calculated from,

$$\eta = {mc(T_o - T_i)}\Big/{IA_a} \tag{16}$$

Calibrated k-type (make: LUTRON TM – 902C) digital thermocouple has been used to measure the absorber surface temperature, glass cover temperature and storage tank temperature. Also calibrated PT (RTD Type) – 100 sensor (make: SELECTRON 303) has been used to measure the outlet temperature of the water. Thermocouples are connected to a digital meter with LED display to record their outputs.

The uncertainties in the measured data were calculated based on the procedure given by Singh et al. [14]. The uncertainty in measurement of temperature and solar intensity are ±0.25% and ± 5% respectively. The uncertainty in experimental thermal efficiency of the solar collector was estimated to be about ±5.5%. All care was taken to reduce manufacturing and assembling error to achieve the concentration ratio.

Design of Trapezoidal Cavity Absorber

Figures 3 (a) and (b) represent the arrangement of the trapezoidal cavity absorber with and without plate underneath the absorber tubes. A set of a six copper round tubes (outer diameter, d_o = 15.8 mm, inner diameter, d_i = 12.7 mm and length, l = 1m) brazed together in a single layer 96mm wide is placed over a copper absorber plate of 120mm width for the first model of cavity with plate (Figure 3(a)). For the second model of cavity without plate, absorber tubes, with same dimension as the first model, are placed without the plate (Figure 3(b)). The absorber surface is coated with black chrome selective surface by the process of electroplating. Thickness of the black chrome plating is about 12μm. A glass cover of width 196mm is placed at the bottom of the cavity 45 mm (De) below the absorber surface to suppress the heat loss from the absorber surface. The insulation thickness of approximately 35mm is placed on the top and two sides of the cavity.

Then, the overall heat transfer coefficient of the absorber surface is determined experimentally at different water temperatures by maintaining different water flow rates. The overall heat loss coefficient of the

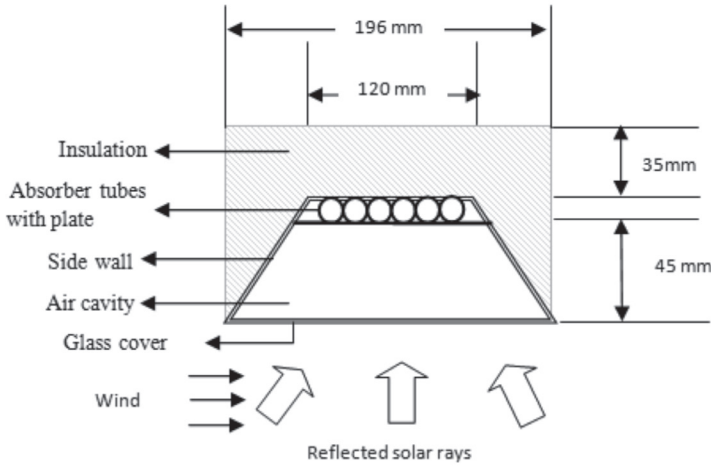

(a)

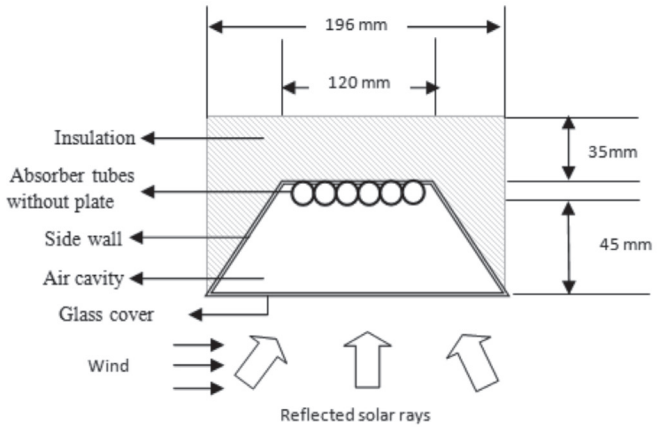

(b)

Figure 3. Sketch of trapezoidal cavity absorbers for analytical modeling; (a) with plate (b) without plate

absorber surface is given by, for cavity with plate,

$$U_l = \left[mc(T_i - T_o)\right] \Big/ A_p(T_p - T_a) \tag{17}$$

where T_p = Absorber plate surface temperature in °C.
And for cavity without plate,

$$U_l = \left[mc(T_i - T_o)\right] \Big/ A_r(T_s - T_a) \tag{18}$$

where T_s = Absorber tube surface temperature in °C.

Several observations are taken at different water temperatures and the water temperature variation from inlet to outlet is within 2 to 7°C.

ANALYTICAL MODELING

Heat transfer in the trapezoidal cavity absorber from hot absorber surface (Figures 3(a) and (b)) is mainly through convection and radiation. The trapezoidal cavity absorber (Figure 4) is insulated (with glass wool) from three sides to reduce heat loss, there would be heat loss from the cavity absorber through insulated sides by conduction and it is considered as negligible in the present analytical model. The natural convection type heat transfer occurs inside the cavity. The radiation heat exchange between the hot absorber surface and the glass cover of the cavity absorber may be taken as the heat transfer between two horizontal parallel surfaces with different temperature. Estimation of the overall heat loss coefficient of the cavity absorber is done by considering convection and radiation losses from the absorber surface (either plate or tube surface) through glass cover to the surroundings [16],

$$1/U_l = \left[1/(h_{cp} + h_{rp}) + (A_p / A_c)\{1/(h_{co} + h_{ro})\}\right] \tag{19}$$

The heat loss between the absorber surface and inner glass surface can be estimated by considering heat loss between two horizontal parallel surfaces (hot surface up and cold surface down). The convection heat transfer correlations, for cavity with plate [26, 27], are given as:

$$h_{cp} = Nu_{cp} K / D_e \tag{20}$$

where,

$$Nu_{cp} = 0.163 Gr^{0.196} \left(\frac{D_e}{W}\right)^{0.316} \tag{21}$$

and for cavity without plate [28],

$$Nu_{cp} = C(Ra)^z \tag{22}$$

in which C and z are constants and are taken from data book [27], according to the range of the value of the Rayleigh number. Physical properties of air have been taken at the average temperature of bottom glass cover and absorber surface. Similarly heat loss at outer cover surface 'h_{co}' can be estimated by [28],

$$h_{co} = 8.55 + (2.56 \times V_w) \tag{23}$$

Radiation losses from a body mainly depend upon body temperature and surface emissivity. Radiation heat transfer coefficient (h_{ro}) from bottom glass cover of the cavity to the ambient can be calculated as [18],

$$h_{ro} = \sigma \varepsilon_c (T_c^2 + T_a)(T_c + T_a) \tag{24}$$

Radiation heat transfer coefficient between hot absorber surface and glass cover (h_{rp}) can be calculated by [18],

$$h_{rp} = [\sigma (T_p^2 + T_c^2)(T_p + T_c)]/[(1/\varepsilon_c) + (1/\varepsilon_p) - 1] \tag{25}$$

The heat loss coefficient is estimated using the measured values of absorber surface temperature (T_p or T_s), cover temperature (T_c) and ambient temperature (T_a) by a MATLAB computer program.

RESULTS AND DISCUSSION

Performance Parameters of the System

In the present work, the various design parameters considered are shift (s), width of reflector (w), location of each reflector (R), height of the absorber plane (f). A program is developed to calculate the concentrated power by using the design parameters. The total concentrated power of the system is found out by using Equations (13) and (15). The maximum concentrated power is obtained as 2.5kW for the value of w = 0.04m, f = 1.1m for a set of 40 numbers of reflectors on either side of concentrator.

By using the above value of f and w, a MATLAB program has been developed to calculate the total concentrated power for different sets (N =10, 20, 30, 40, 50, etc.) of glass reflectors with reflectivity of 0.98. The reflectivity of the glass was measured out by using Novo – Glass (Statistical Glassmeter), Komal Scientific Co., India. The variation of

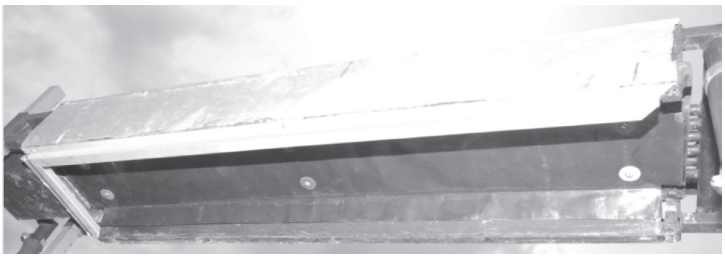

(a)

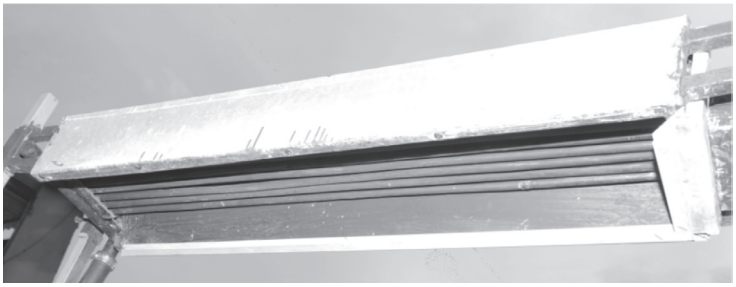

(b)

Figure 4. Trapezoidal cavity absorbers without bottom glass cover (a) with plate (b) without plate

concentrated power with respect to number of reflectors (N) is shown in Figure 5. The concentrated power is observed to increase with number of reflectors up to about 40. The extra-axial reflector mirrors beyond N = 40 contributed little to the concentrated power due to the larger cosine losses associated with them.

Figure 6 shows the graph between total number of mirror reflector and the concentration ratio. The growth of the concentration ratio declines slowly with increase in the number of reflectors. Gain in concentration ratio reduced significantly with increasing number of reflector mirrors after concentration ratio of 19. This may be attributed to the cosine effect of the reflector angle (θ_n) as the contribution of the nth mirror reflector to the concentration ratio depends upon the factor Cos θ_n (Equation (6)).

The distribution of the local concentration ratio on the absorber of the present LFRSC system with the distance along the absorber plane is plotted in Figure 7. It may be seen that a uniform concentration ratio (22.44) is obtained over a width (70 mm) of the absorber plane and there-

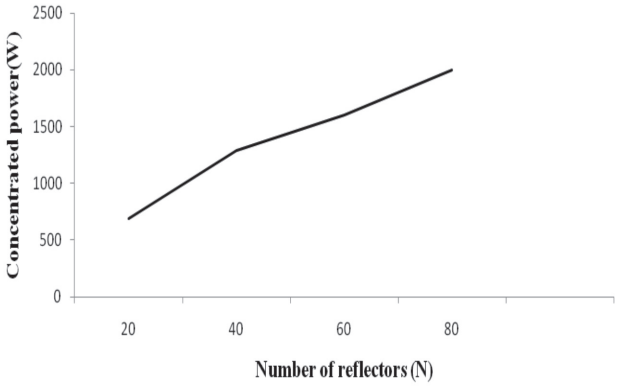

Figure 5. Number of mirrors Vs Concentrated power

after the concentration gradually falls down to zero. The observation is found in line with the literature results [14, 25, and 29]. Hence in the present LFRSC system, out of six tubes, almost five tubes (each of which has 15.6mm OD) located at the center of the absorber plane receive same radiation. So, the central tube temperature is measured and assumed as the mean absorber surface temperature for heat transfer analysis.

Temperature Analysis

The experiment is conducted for three different mass flow rates (0.03, 0.025 and 0.02 kg/s) in two cavity models on clear sunny days. The observations are made during the month of July, 2012. The capacity of water storage tank is 15 litres. The values of the storage tank temperature (T_{tank}), collector water inlet (T_i) and outlet (T_o) temperatures, absorber surface temperature (T_p or T_s), bottom glass temperature (T_g)

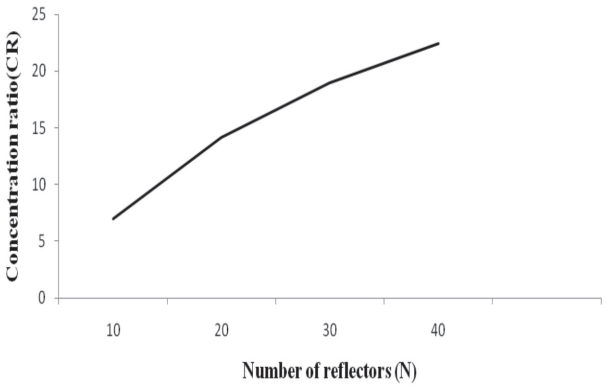

Figure 6. Number of mirrors Vs Concentration ratio

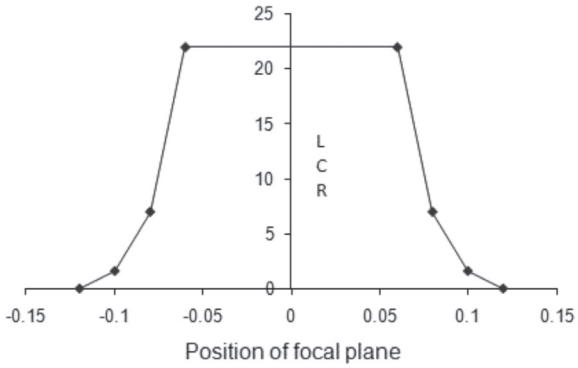

Figure 7. Distribution of local concentration ratio on the absorber plane

and ambient temperature (T_a) are shown in Tables 1 and 2 for the trapezoidal cavity with and without plate respectively. It is found that the temperature of water was tending to rise rapidly in all cases during start up. However it reached the stagnant value around 2.00 pm to 3.00 pm. Also, it is seen that the time required for reaching this peak stagnant value is less for trapezoidal cavity with plate as compared to trapezoidal cavity without plate. This may be attributed to lower heat loss coefficient values in cavity with plate as compared to that of cavity without plate. From Tables 1 and 2, it is also inferred that the peak stagnant temperature values reduced by reducing the mass flow rate of the system.

The range of variation in the storage tank temperature is from 38°C to 72°C for the cavity with plate at different mass flow rates as compared to 38°C to 65°C for the cavity without plate. Regarding the outlet temperature of the water at 0.02kg/s from the cavity absorber tubes, a maximum of 73°C for the cavity with plate and 66°C for the cavity without plate is achieved. Also from the experimental analysis, it is identified that, the maximum difference between the inlet and outlet temperature in the absorber tubes is 7°C for the cavity with plate and 4°C for the cavity without plate. As expected, this decrease in temperature difference is due to the higher heat loss coefficient for the cavity without plate at bottom. So, from the Table 1 and 2, it is observed that, the cavity with plate gives higher outlet water temperature and storage tank temperature at all mass flow rates as compared to cavity without plate. The range of variation of temperature from inlet to outlet header is in line with the results as shown in literature [29].

Table 1: Various temperature obtained for the cavity with plate at the mass flow rate of (a) 0.03kg/s (b) 0.025 kg/s (c) 0.02 kg/s

Time	T_{tank} (^{0}C)	T_i (^{0}C)	T_o (^{0}C)	T_p (^{0}C)	T_c (^{0}C)	T_a (^{0}C)	I (W/m^2)
10.00 am	38	34	36	110	85	35	689.01
11.00 am	41	36	40	135	98	36	811.53
12.00 pm	50	44	48	158	130	35	816.2
1.00 pm	58	51	56	168	135	36	1233.16
2.00 pm	62	54	60	160	130	36	1027.84
3.00 pm	65	58	60	110	86	34	981.5
4.00 pm	65	62	65	95	76	33	736.9

(a)

Time	T_{tank} (^{0}C)	T_i (^{0}C)	T_o (^{0}C)	T_p (^{0}C)	T_c (^{0}C)	T_a (^{0}C)	I (W/m^2)
10.00 am	38	36	40	128	85	35	862.46
11.00 am	42	39	43	135	98	37	1166.21
12.00 pm	52	48	53	135	113	37	1283.9
1.00 pm	60	57	61	170	138	38	1091.32
2.00 pm	66	62	67	160	133	34	1176.6
3.00 pm	68	65	67	103	88	34	848.6
4.00 pm	68	65	66	90	73	33	628.9

(b)

Time	T_{tank} (^{0}C)	T_i (^{0}C)	T_o (^{0}C)	T_p (^{0}C)	T_c (^{0}C)	T_a (^{0}C)	I (W/m^2)
10.00 am	38	36	38	84	63	38	879.81
11.00 am	42	39	43	130	87	37	951.72
12.00 pm	52	50	54	140	112	34	1246.8
1.00 pm	63	60	65	155	118	36	1202.9
2.00 pm	72	70	71	125	110	38	1062.6
3.00 pm	71	69	70	110	88	36	961.4
4.00 pm	71	69	70	90	74	33	626.15

Overall Heat Loss Coefficient

Experimental Analysis

The experimental values of the overall heat loss coefficient of cavity absorber with and without plate (Figure 8) for black chrome coated varied with absorber surface temperature are obtained by using Equations (17) and (18). Range of overall heat loss coefficients in the two different trapezoidal cavity absorber is given in Table 3 and it lies in the range of 4.3 to 5.8 W/m^{2}K for trapezoidal cavity absorber with plate as compared to 5.4 to 6.8 W/m^{2}K for without plate. It can be seen that

the cavity absorber with plate and black chrome coating has lower heat loss coefficient values as compared to cavity absorber without plate and black chrome coating. This experimental result is in agreement with the numerical result reported in literatures [16, 17, and 30]. This may be due to the absorber surface area exposed to the cavity air is slightly more for trapezoidal cavity without plate as compared to cavity with plate. Also, it is noted that the difference between overall heat loss coefficient of cavity absorber surface with and without plate are more at lower absorber

Table 2: Various temperature obtained for the cavity without plate at the mass flow rate of (a) 0.03kg/s (b) 0.025 kg/s (c) 0.02 kg/s

Time	T_{tank} (^{0}C)	T_i (^{0}C)	T_o (^{0}C)	T_s (^{0}C)	T_c (^{0}C)	T_a (^{0}C)	I (W/m^2)
10.00 am	38	37	38	97	92	34	1150.8
11.00 am	45	44	48	114	105	35	1170
12.00 pm	56	52	56	110	98	36	1397.56
1.00 pm	62	57	64	110	88	37	1339.78
2.00 pm	64	62	67	105	87	39	1248.28
3.00 pm	64	62	64	98	76	35	1056.6
4.00 pm	64	62	63	89	75	32	290.65

(a)

Time	T_{tank} (^{0}C)	T_i (^{0}C)	T_o (^{0}C)	T_s (^{0}C)	T_c (^{0}C)	T_a (^{0}C)	I (W/m^2)
10.00 am	39	37	38	123	88	33	775.2
11.00 am	46	44	48	134	98	35	1083.6
12.00 pm	57	54	57	135	113	35	1081.2
1.00 pm	63	60	64	170	138	36	945.03
2.00 pm	65	62	66	159	135	38	1098.7
3.00 pm	65	62	64	103	90	35	859.73
4.00 pm	65	62	63	92	73	32	650.9

(b)

Time	T_{tank} (^{0}C)	T_i (^{0}C)	T_o (^{0}C)	T_s (^{0}C)	T_c (^{0}C)	T_a (^{0}C)	I (W/m^2)
10.00 am	39	37	38	84	63	38	882.3
11.00 am	48	44	48	131	88	37	1050.9
12.00 pm	58	54	57	131	108	34	1153.3
1.00 pm	63	60	64	154	123	36	1319
2.00 pm	66	65	67	127	110	38	1222.25
3.00 pm	66	64	65	101	88	36	862.21
4.00 pm	66	64	65	85	74	33	595.9

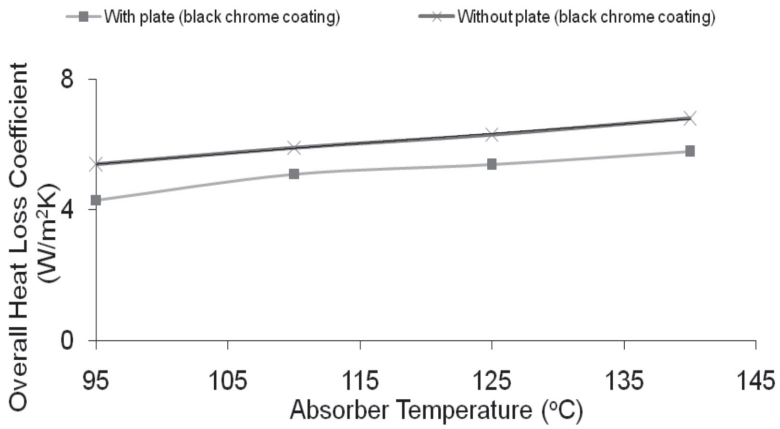

Figure 8. Comparison of overall heat loss coefficient for the cavity absorber with and without plate

Table 3:
Overall heat loss coefficient for cavity absorber with and without plate

Cavity absorber type	Overall heat loss coefficient (W/m^2K)
With plate	4.3-5.8
Without plate	5.4-6.8

surface temperature (at 95°C) and slowly the difference is getting lower at higher temperatures.

Analytical and Experimental Comparison

Figure 9 shows the effect of absorber temperature on the overall heat loss coefficient of cavity with plate for analytical and experimental values. The trend of variation of overall heat loss coefficient of analytical values is similar to the experimental values i.e. the overall heat loss coefficient increases with increase in absorber surface temperature. This may be due to the fact that convection and radiation heat loss increases with temperature particularly the radiation heat loss. The overall heat loss coefficient values obtained by experimental method are 10-14% lower than the analytical results. The magnitude of error depends on the particular combination of the radiative parameters used and assumptions (as described in section 3) made in the analytical models.

Figure 10 shows the effect of absorber temperature on the experimental and analytical values of the overall heat loss coefficient for the

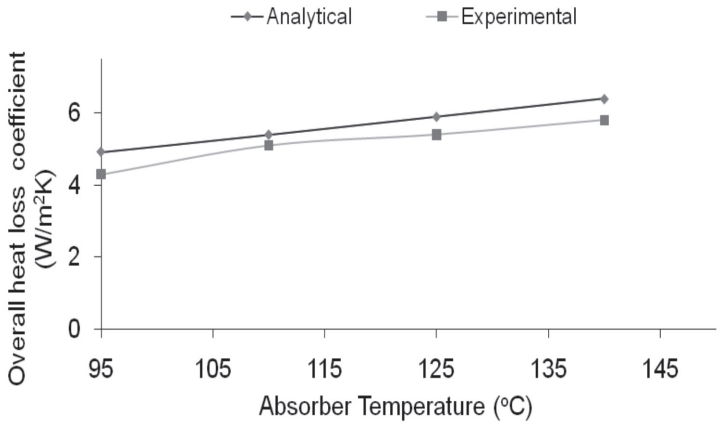

Figure 9. Effect of absorber temperature on the overall heat loss coefficient for the cavity with plate

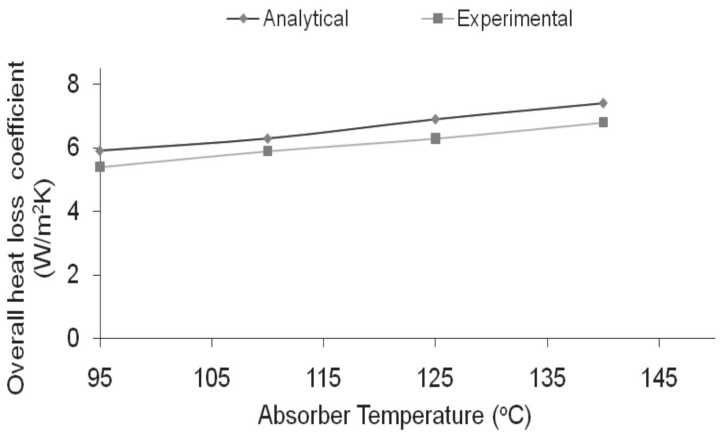

Figure 10. Effect of absorber temperature on the overall heat loss coefficient for the cavity without plate

cavity without plate and black chrome coating. In this case also, the overall heat loss coefficient increases with absorber temperature values. The deviations of experimental values of the heat loss coefficient from the analytical ones are slightly less to the analytical values as compared to cavity with plate (Figure 9). The experimental values are 8.8-9.6% lower than analytical values.

In the present study, the heat loss coefficient estimated by analyti-

cal method is over predicted by 8.8-14% as compared to the experimental values. Over prediction of the absorber heat loss to the experimental values is quite acceptable from the design point of view [30]. Also, the percentage variation of present experimental values with the analytical values is lesser as compared to percentage variation (10% - 40%) reported in earlier works [16, 26].

Correlation Analysis

In this section, the correlation between the overall heat transfer coefficient and the absorber temperature for two different cavity models is developed. The power-law fit trend line has been chosen to correlate to the results. The power curve between heat loss coefficient and absorber temperature is found to be best fit with correlation coefficient (R^2) of about 0.98 on an average. Similar observations (0.9) were also made by [20]. The general relation between overall heat loss coefficient and absorber surface temperature can be given by [16], for the cavity with plate,

$$U_l = G(T_p)^d \tag{26}$$

for the cavity without plate,

$$U_l = G(T_s)^d \tag{27}$$

where coefficient G and index d are constant.

The overall heat loss coefficient is predicted for cavity absorber with and without plate with the correlations developed for the respective absorbers with help of Equations (26) and (27). Good agreement between analytical and experimental values is observed. Deviation between experimental and predicted correlated values is within 5% to 12% in case of cavity absorber with plate and within 10% to 14% in the case of cavity absorber without plate. This trend is similar to the results found in literatures [22]. Values of the constant R^2, G and d obtained for correlation equation for different absorber temperature for the considered models are given in Table 4.

Efficiency of the System

Thermal efficiency of the LFRSC system is mainly influenced by mass flow rate, surface coating on the absorber pipe, concentration ratio

Table 4: Values of the constants R2, G and d for predicted and experimental results

Model	Analysis type	R^2	G	D
Cavity with plate	Analytical	0.99	0.20	0.67
	Experimental	0.96	0.14	0.74
Cavity without plate	Analytical	0.99	0.45	0.36
	Experimental	0.99	0.37	0.58

of the concentrator, water inlet temperature, ambient temperature and solar intensity. The thermal efficiency for both the trapezoidal cavity absorbers with and without plate is calculated experimentally by using Equation (16). For the comparison of the two cavity models, the efficiency of the LFRSC system is determined for three different mass flow rates, viz. 0.03, 0.025 and 0.02kg/s. The performance curve for efficiency Vs time for the three different mass flow rates is plotted to understand the effect of variation of solar intensity (time) and mass flow rate on efficiency of the LFRSC system for the two cavity models (with and without plate). Figures 11 and 12 show the range of thermal efficiency obtained for cavity with and without plate for black chrome coating at different mass flow rates with respect to time. Thermal efficiency of selective surface black chrome coated cavity with plate is found to be 9.1% to 32% as compared to 9% to 26% cavity without plate. The use of trapezoidal cavity with plate, however, results in a considerable improvement in the thermal efficiency as compared to cavity without plate. Higher thermal

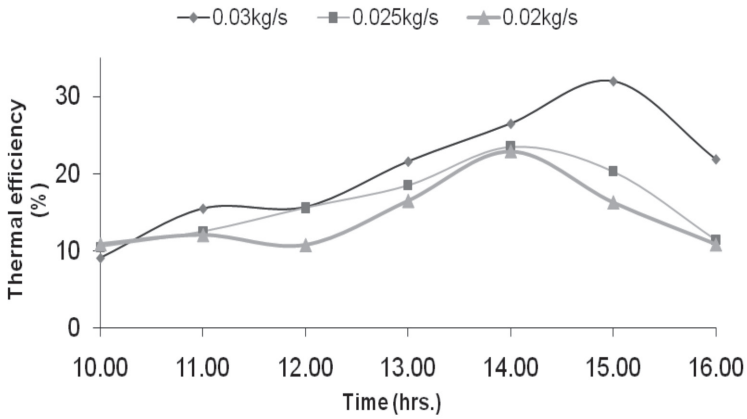

Figure 11. Thermal efficiency Vs Time for the cavity with plate at different mass flow rate

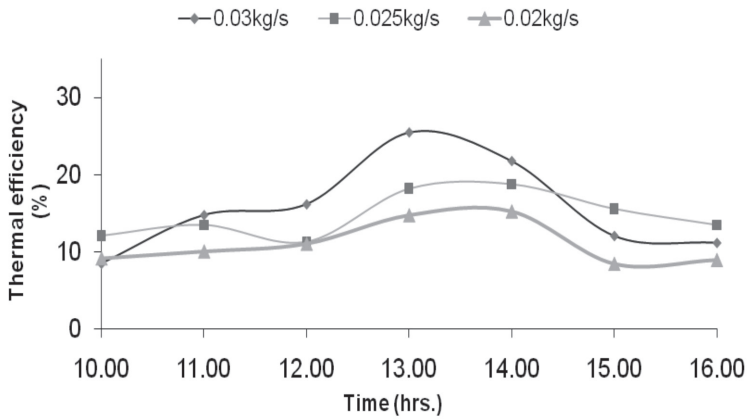

Figure 12. Thermal efficiency Vs Time for the cavity without plate at different mass flow rate

efficiency in the cavity with plate may be due to reduction in overall heat loss coefficient as discussed earlier.

The thermal efficiency of LFRSC system also decreases with decrease in mass flow rate. This may be due to the increase in heat loss with the rise in temperature at the focus due to reduced mass flow rate. It is inferred that the maximum efficiency is obtained at mass flow rate of 0.03kg/s for both the trapezoidal cavities (with and without plate) and lower efficiency at the mass flow rate of 0.02kg/s. Also, the thermal efficiency of the system is high at 12.00 to 14.00 hrs for both the cavity models. The obtained values ranged from 9% to 32%, which is in the range of other values found in the literature [14, 29].

Figure 13 shows the thermal efficiency curves plotted against the factor $(T_i - T_a)/I$ at the optimum mass flow rate (0.03 kg/s) of the present LFRSC system for cavity with and without plate. It is seen that the thermal efficiency decreased with the increase in the factor $(T_i - T_a)/I$. Similar trend is seen in the literatures [14, 29]. Observation of the curves also revealed that smaller the temperature difference $(T_i - T_a)$and higher the solar intensity (I), higher was the collector efficiency. The maximum efficiency occurred at the condition where inlet fluid temperature is almost same as the ambient temperature. This is attributed to lower heat loss from the absorber at inlet water temperature near to ambient. On the other hand, low collector efficiencies are the result of low radiation levels and high fluid inlet temperatures. This would be due to higher

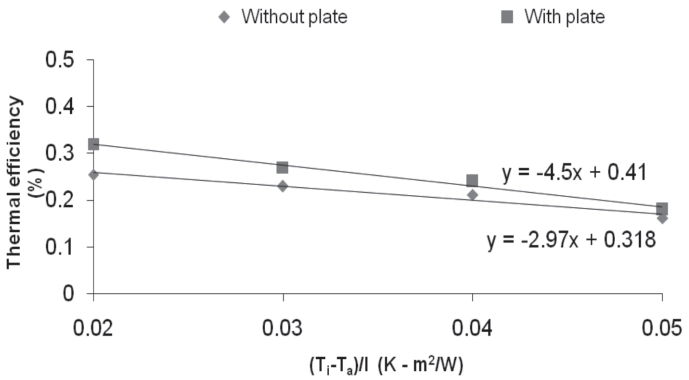

Figure 13. Thermal efficiency Vs (Ti-To)/I for the cavity absorber

heat loss from the absorber at higher inlet temperature. Also from Figure 13, it is inferred that use of cavity with plate resulted in considerable improvement in the thermal efficiency of the concentrator–receiver system. The trapezoidal cavity absorber with plate maintained 26.9% higher efficiency as compared to that of cavity absorber without plate at the optimum mass flow rate.

The regression curve between thermal efficiency of the LFRSC and the factor $(T_i - T_a)/I$ is linear. It is in line with the curve obtained for solar collector analyzed in literatures [14, 31]. The relationship between the thermal efficiency and $(T_i - T_a)/I$ may be expressed as:

$$\eta = k(T_i - T_a)/I + l \tag{28}$$

Where, 'k' and 'l' are constants. Constant 'k' is slope of the straight line and 'l' is intercept on Y-axis. The best fit curve is linear equation for both slope and intercept. Also, the regression line constants 'k' and 'l' values are shown in Figure 13.

CONCLUSIONS

A comparison of combined natural convection and surface radiation model for the two solar trapezoidal cavity absorber models (with and without plate) of LFRSC was presented. The overall heat loss coefficient of the cavity absorber increases with absorber temperature. Values of the heat loss coefficient for different trapezoidal cavity absorbers were

predicted as 4.3 - 8.1W/m^{2}K. The values of the heat loss coefficient for the trapezoidal cavity absorber were slightly higher as compared to the values presented in literatures [16, 20]. The cavity with plate was found to be more efficient as compared to cavity without plates. The values of the constants for the power law correlation have been derived from the analytical and experimental results for both the cavity models. The trend of variation of overall heat loss coefficient estimated with analytical model was similar to the experimental values. Good agreement (within 14%) between predicted analytical values and experimental values were observed. Also from the experimental analysis, it is identified that, the maximum difference between the inlet and outlet temperature in the absorber tubes is 7°C for the cavity with plate and 4°C for the cavity without plate. Further, the thermal efficiency of the LFRSC system had been analyzed and it decreased with the increase in mass flow rate. The thermal efficiency for cavity absorber with plate ranged from 9.1% to 32% and without plate ranged from 9% to 26%. The present analytical and experimental study of cavity absorber of a LFRSC suggests the use of absorber plate underneath the absorber tubes enhances the thermal performance of cavity absorber and hence the LFRSC system.

References

[1] Di Canio DG, Tretyl WJ, Jur FA, Watson CD. Line-focus Solar Thermal Central Receiver Research Study. FMC Corporation, Santa Clara, CA, Final Report. Available at http://www.osti.gov/energycitations/product.biblio.jsp?osti_id¼ 5535434; 1977.
[2] Vant-Hull LL. In: Winter CJ, Sizmann RL, Vant-Hull LL, editors. Solar power plants. Berlin: Springer-Verlag; 1991. p. 114.
[3] Nixon JD, Dey PK, Davies PA. Which is the best solar thermal collection technology for electricity generation in north-west India? Evaluation of options using the analytical hierarchy process. Energy 2010;35: 5230-5240.
[4] Feuermann D, Gordon JM. Analysis of a two-stage linear Fresnel reflector solar concentrator. ASME Journal of Solar Energy Engineering 1991;113:272-79.
[5] Feuermann D. Analysis and Evaluation of the Solar Thermal System at the Ben-Gurion Sede Boqer Test Center for Solar Electricity Generating Technologies. Israel Ministry of Energy and Infrastructure, Jerusalem. Final Report, Contract No. 88169101, July 2003.
[6] Kalogirou, S. Solar thermal collectors and applications. Progress in Energy and Combustion Science 2004;30:231-95.
[7] Mills D, Morrison GL. Compact linear Fresnel reflector solar thermal power plants. Solar Energy 2000;68:3:263-83.
[8] Häberle A, Zahler C, Lerchenmüller H, Mertins M, Wittwer C, Trieb Fl. The solarmundo line focussing Fresnel collector. Optical and thermal performance and cost calculations. In: 11th solar PACES international symposium on concentrated solar power and chemical energy technologies; 2002. Sept. 4-6, Zurich, Switzerland.
[9] http://www.spg-gmbh.com; Solar Power Group 2008.

[10] http://www.ausra.com; Ausra 2009.
[11] Hoshi A, Mills DR, Bittar A, Saitoh TS. Screening of high melting point phase change materials (PCM) in solar thermal concentrating technology based on CLFR. Solar Energy 2005;79:332-39.
[12] Roberto Grena, Pietro Tarquini. Solar linear Fresnel collector using molten nitrates as heat transfer fluid. Energy 2011;36:1048-56.
[13] Jance MJ, Morrison GL, Behnia M. Natural convection and radiation within an enclosed inverted absorber cavity: preliminary experimental results. International Renewable Energy Transforming Business: proceedings of solar. 2000; Brisbane: ANZSES.
[14] Singh PL, Sarviya RM, Bhagoria JL. Thermal performance of linear Fresnel reflecting solar concentrator with trapezoidal cavity absorbers. Applied Energy 2010 a;87:541-50.
[15] Flores Larsen S, Altamirano A, Hernandez A. Heat loss of a trapezoidal cavity absorber for a linear Fresnel reflecting solar concentrator. Renewable Energy 2012;39:198-206.
[16] Singh PL, Sarviya RM, Bhagoria JL. Heat loss study of trapezoidal cavity absorbers for linear solar concentration collector. Energy conversion and Management 2010 b;51: 329-37.
[17] Natarajan E, Basak T, Roya S.Natural convection flows in a trapezoidal enclosure with uniform and non-uniform heating of bottom wall. International Journal of Heat and Mass Transfer 2008;51(3-4):747–56.
[18] Chapman AJ. Heat transfer. New York: Macmillan Publishing House; 1984.
[19] Balaji C, Venkatesan S. Correlations for free convection and surface radiation in square cavity. International Journal of Heat and Fluid Flow 1994;15(3):249–51.
[20] Facao Jorge, Armando Oliveria C. Numerical simulation of a trapezoidal cavity receiver for a linear Fresnel solar collector concentrator. Renewable Energy 2011;36:90-96.
[21] Sendhil Kumar Natarajan, Reddy KS, Tapas Kumar Mallick. Heat loss characteristics of trapezoidal cavity receiver for solar linear concentrating system. Applied Energy 2012;93: 523-31.
[22] Manikumar R, Valan Arasu A, Jayaraj S. Numerical simulation of a trapezoidal cavity absorber in the linear Fresnel reflector solar concentrator system, International Journal of Green Energy. http://dx.doi.org/10.1080/15435075.2012.752375.
[23] ANSYS workbench 12.0, FLUENT 12.0, User's guide, 2009.
[24] Manikumar R, Valan Arasu A. Design and theoretical performance analysis of linear Fresnel reflector solar concentrator with a tubular absorber. International Journal of Renewable Energy Technology 2012;3(3):221-36.
[25] Negi BS, Kandpal TC, Mathur SS. Designs and performance characteristics of a linear Fresnel reflector solar concentrator with a flat vertical absorber. Solar Wind Technology 1990;7(4):379-92.
[26] Reynolds DJ, Jance MJ, Behnai M, Morrison A. An experimental and computational study of the heat loss characteristics of a trapezoidal cavity absorber. Solar Energy 2004;76: 229–34.
[27] Kothandaraman CP, Subramanyan S. Heat and Mass Transfer Data Book. New Delhi: New Age International Publishers; 2008.
[28] Sukhatme SP, Nayak JK. Solar energy principles of thermal collection and storage. New York: Tata McGraw-Hill Publication; 2009.
[29] Negi BS, Mathur SS, Kandpal TC. Optical and thermal performance evaluation of a linear Fresnel reflector solar concentrator, Solar and Wind Technology, 1989;6(5):

589-593.
[30] Manikumar R, Valan Arasu A, Jayaraj S. Computational fluid dynamics analysis of a trapezoidal cavity absorber used for the linear Fresnel reflector solar concentrator system, Journal of Renewable and Sustainable Energy, 2012;4: 063145 (1-18).
[31] Valan Arasu A, Sornakumar TD. Performance characteristics of parabolic trough solar collector system, Int Energy J, 2006;7:137–45.

ABOUT THE AUTHORS

R. Manikumar (corresponding author) is an Assistant Professor, Department of Mechanical Engineering of Kamaraj College of Engineering and Technology (TN), India. He holds Bachelor's degree in Mechanical Engineering and Master's degree in Thermal Engineering. He is pursuing his PhD at Anna University of Technology, Tirunelveli, Tamil Nadu, India. He has eight years of teaching experience. He has published three numbers of technical papers in referred international journal and six numbers in referred national level journal. He has got prestigious "Young Scientist Fellowship Award 2012" from Tamil Nadu State Council for Science and Technology, Government of Tamil Nadu, India. Also he has carried out one sponsored technical project work. Contact information: R. Manikumar, Assistant Professor, Department of Mechanical Engineering, Kamaraj College of Engineering and Technology, S.P.G.C. Nagar, Virudhunagar – 626001, Tamil Nadu, India. e-mail: mani2k72006@yahoo.co.in. Phone: 00 + 91 - 04549- 278171.

Dr. A. Valan Arasu is an Associate Professor, Department of Mechanical Engineering of Thiagarajar College of Engineering, Madurai, India. He obtained his Bachelor's degree in Mechanical engineering First class with Distinction from Thiagarajar College of Engineering, Madurai, India and both Master's degree in Thermal engineering First class with Distinction and Ph.D. degree from Anna University, Chennai, India. He completed PDF in the area of phase change materials at NUS, Singapore under BOYSCAST fellowship from Department of Science and Technology, Government of India. He has published many technical papers in refereed International Journals and Conferences and carried out several sponsored technical project works.